ACS Macro Letters

pubs.acs.org/macroletters Letter

Electrostatic Repulsion Slows Relaxations of Polyelectrolytes in Semidilute Solutions

Ali H. Slim, Winnie H. Shi, Farshad Safi Samghabadi, Antonio Faraone, Amanda B. Marciel,* Ryan Poling-Skutvik,* and Jacinta C. Conrad*

Cite This: ACS Macro Lett. 2022, 11, 854−860 Read Online

ACCESS | Metrics & More | Article Recommendations | Supporting Information

ABSTRACT: We investigate the structure and dynamics of unentangled semidilute solutions of sodium polystyrenesulfonate (NaPSS) using small-angle neutron scattering (SANS) and neutron spin−echo (NSE) spectroscopy. The effects of electrostatic interactions and chain structure are examined as a function of ionic strength and polymer concentration, respectively. The SANS profiles exhibit a characteristic structural peak, signature of polyelectrolyte solutions, that can be fit with a combination of a semiflexible chain with excluded volume interactions form factor and a polymer reference interaction site model (PRISM) structure factor. We confirm that electrostatic interactions vary with ionic strength across solutions with similar geometries. The segmental relaxations from NSE deviate from theoretical predictions from Zimm and exhibit two scaling behaviors, with the crossover between the two regimes taking place around the characteristic structural peak. The chain dynamics are suppressed across the length scale of the correlation blob, and inversely related to the structure factor. These observations suggest that the highly correlated nature of polyelectrolytes presents an additional energy barrier that leads to de Gennes narrowing behavior.

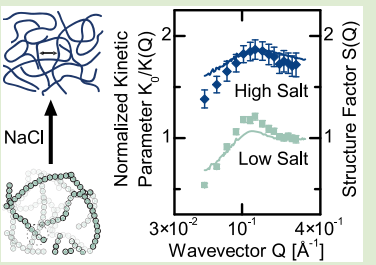

The mechanical response of polyelectrolytes is primarily determined by the chain dynamics,[1] which in turn is dictated by the configuration of polyelectrolyte chains. Electrostatic interactions on the polyelectrolyte backbone affect the chain conformation. Additionally, these interactions underpin the favorable properties that make polyelectrolytes an essential component of biological systems such as cartilage tissues[2−4] and good lubricants for muscle joints[5] and as thickening agents and rheological modifiers in cosmetics,[6,7] food products,[8,9] and paints.[10] Hence, understanding the effects of structure on the dynamics of polyelectrolyte solutions is key to identifying and controlling the distinct physical processes governing the mechanics of polyelectrolyte solutions.

The structure of polyelectrolytes deviates strongly from predictions for neutral chains[11,12] because of the electrostatic repulsions along the polymer backbone.[13−16] These interactions result in a highly extended conformation of electrostatic blobs inside the correlation blob.[12,14,17−19] On length scales beyond the correlation volume, polyelectrolytes transition to a random walk conformation of correlation blobs as the repulsive interactions are screened.[12,14,18] Alternatively, these interactions can be screened at high ionic strengths so that polyelectrolytes approach fully flexible chain conformations. These unique structural properties have significant effects on chain dynamics, as reported by studies exploring the effects of counterion valence,[20] electrostatic screening length scaling,[21] and entanglement crossover and density.[22] The segmental relaxations of neutral chains are described by the Zimm model in dilute solutions,[23] by the Rouse model in semidilute solutions,[24] and by the reptation model in entangled solutions.[25] Experimental measurements of viscosity, relaxation times, and disentanglement,[22,26−34] however, show poor agreement with scaling model predictions for polyelectrolytes. We expect these discrepancies are caused by the extended structure of the polyelectolyte chains. Therefore, there is a critical need to independently measure polyelectrolyte conformation and segmental relaxations to elucidate the relationship between structure and dynamics in semidilute polyelectrolyte solutions.

In this study, we show that the segmental relaxations of polyelectrolytes follow de Gennes narrowing in which the local chain structure perturbs standard Zimm relaxations. We independently tune geometric and electrostatic length scales, measured with small-angle neutron scattering (SANS), by varying polymer and salt concentrations, respectively, to understand the dynamic behavior of polyelectrolytes, measured with neutron spin echo (NSE) spectroscopy. The SANS profiles of these solutions at all ionic strengths resemble the profile expected for chains with highly extended random walk conformation and can be fit using a model combining the form factor of a semiflexible chain with excluded volume interactions and a PRISM structure factor. Chain dynamics across the

Received: April 5, 2022
Accepted: June 21, 2022

https://doi.org/10.1021/acsmacrolett.2c00213
ACS Macro Lett. 2022, 11, 854−860

correlation length ξ, however, deviate from the standard Zimm model. Specifically, the polymer dynamics are suppressed around the structure peak induced by the electrostatic interactions between chains. Approximating the structure factor of the polyelectrolyte chains as a perturbation from Gaussian chains, we demonstrate that these slow relaxations are wholly described by the structure of polyelectrolytes and follow the theoretical prediction of de Gennes narrowing, in which dynamics are inversely related to structure due to the presence of a free energy minimum over a characteristic structural length scale.[35,36] Our findings indicate that the unique structural properties of charged chains underpin the deviation of polyelectrolyte dynamics from theoretical predictions.

Our experimental system consists of sodium polystyrenesulfonate (NaPSS) chains (M_w = 68 kDa) dissolved in Millipore water or deuterium oxide for rheology and neutron scattering experiments, respectively.[37] The ionic strength of the solutions was tuned by adding appropriate amounts of sodium chloride. The radius of gyration was determined from intrinsic viscosity experiments to be $R_{g,0}$ = 13, 12, and 9.5 nm at ionic strengths of $I = 10^{-6}$, 10^{-2}, and 10^{-1} M (M = mol/L, moles per liters of solution), respectively. The polymer concentrations were chosen to obtain similar correlation lengths as ionic strength changes according to de Gennes' scaling predictions $\xi = R_{g,0}(c/c^*)^{-\nu/(3\nu-1)}$. Steady-shear rheology measurements were performed on a Discovery Hybrid Rheometer (TA Instrument, HR-2) using a Couette geometry. We collected small-angle neutron scattering (SANS) and neutron spin−echo (NSE) data on the NGB30 and NSE instruments, respectively, at the Center for Neutron Research, National Institute of Standards and Technology (NIST).[38,39] The raw SANS and NSE data were reduced using IgorPro[40] and DAVE[41] software package, respectively. All experiments were performed at room temperature.

We confirm that the rheology of these solutions follows established predictions for polyelectrolyte solutions (Figure 1).[14,17,22,27,37] At dilute concentrations ($c/c^* < 1$), the specific viscosity $\eta_{sp} = (\eta - \eta_s)/\eta_s$, where η and η_s are the solution and solvent viscosities, respectively, of solutions collapse together due to the dominance of hydrodynamic interactions[23,42,43] with a scaling $\eta_{sp} \sim (c/c^*)^1$. In the semidilute regime ($c/c^* > 1$), η_{sp} increases as a power-law with polymer concentration ($\eta_{sp} \sim (c/c^*)^{\alpha}$) and conforms with the scaling predictions in the limits of low ($\alpha = 1/2$) and high ($\alpha = 5/4$) ionic strength. For solutions of intermediate ionic strength, however, $\alpha = 0.9 \pm 0.1$ is intermediate between the low and high salt limits.

The rheology measurements show that the properties of polyelectrolyte systems can be tuned by screening the electrostatic interactions, which modify the polymer conformations. To characterize these conformations, we capture the scattering profile of our solutions using SANS to quantify their structural properties within the correlation blob. SANS measurements at small length scales allow us to accurately determine the characteristic chain length scales. The SANS scattering profiles of NaPSS solutions display a local maximum at Q^* between (0.08 and 0.14) Å^{-1} (Figure 2a and the SI). The peak is the characteristic structural signature of polyelectrolyte solutions and results from the high osmotic pressure due to counterion entropy, which prevents the overlap of correlation volumes.[12,14] The scattering profiles are well fit using a model that combines the form factor of a semiflexible chain with excluded volume interactions and a PRISM

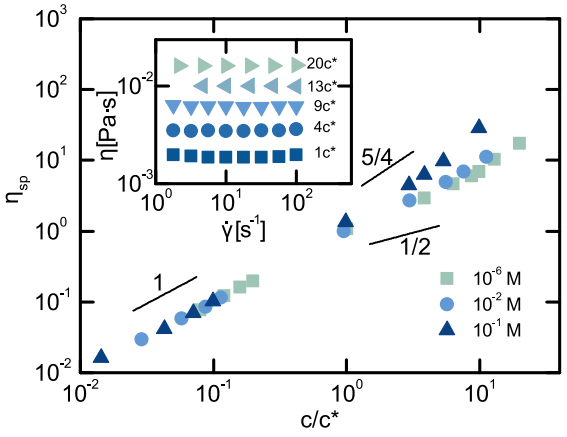

Figure 1. Specific viscosity $\eta_{sp} = (\eta - \eta_0)/\eta_0$ as a function of normalized NaPSS concentration c/c^* for solutions of various ionic strengths. Inset: Viscosity η for 10^{-6} M ionic strength solutions as a function of shear rate $\dot{\gamma}$. Error bars are smaller than symbols and represent the standard deviation of two separate measurements. Polymer solution viscosity remains constant at all shear rates (additional data for 10^{-6}, 10^{-2}, and 10^{-1} in the SI). Bottom and top solid lines represent viscosity scaling predicted for polyelectrolytes in the limit of low and high ionic strength, respectively.

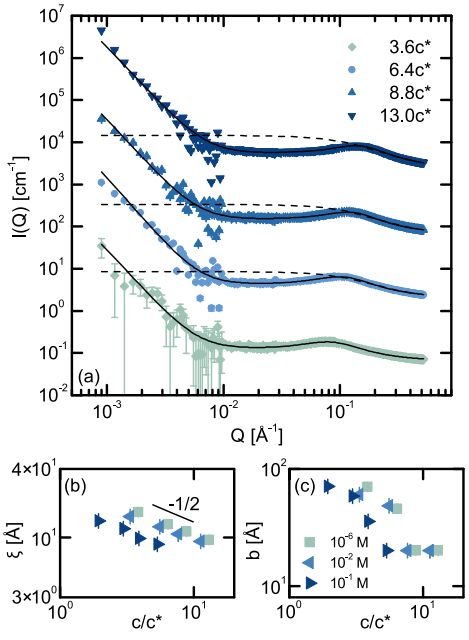

Figure 2. (a) SANS intensity $I(Q)$ as a function of wavevector Q for different concentrations of NaPSS solutions at 10^{-6} M ionic strength. Solid and dashed lines represent fits from eqs 1 and 2, respectively. NSE measurements were not performed at the lowest polymer concentration due to low signal. Data are shifted vertically for clarity. (b) Correlation length ξ and (c) Kuhn length b obtained from fits to eq 1 as a function of polymer concentration c/c^* at various ionic strengths. Solid line in (b) represents theoretical scaling. Error bars are estimated according to a 95% confidence interval.

structure factor.[44−46] The form factor assumes that chains are semiflexible on length scales greater than the persistence length l_p and rod-like at length scales below l_p without accounting for electrostatic contributions. The effects of electrostatic interactions are incorporated by adding the form factor into the PRISM theory expression for the scattering intensity[47−51]. We add an empirical power law term to capture

https://doi.org/10.1021/acsmacrolett.2c00213
ACS Macro Lett. 2022, 11, 854−860

the upturn at low Q due to large scale inhomogeneities.[16] SANS data were fitted using the following equation:

$$I(Q) = k\frac{P(Q, L, b)}{1 + \alpha c(Q, \xi)P(Q, L, b)} + Q^{-m} \quad (1)$$

where k is a scaling factor, L is the contour length of the chain and is fixed at 580 Å (SI), α is inversely related to the osmotic compressibility,[52] and m is the $I(Q)$ slope at low Q. The functional forms for $c(Q, \xi)$ and $P(Q, L, b)$ are provided in the SI.

The structural parameters obtained from SANS fits follow the expectations for polyelectrolyte solutions (Figure 2b). With increasing polymer concentration, the electrostatic screening of backbone functional groups by counterions increases, resulting in a power-law decrease of $\xi \sim (c/c^*)^{-1/2}$, consistent with theoretical predictions.[14,27] At all polymer and salt concentrations, the effective Kuhn length is larger than or equal to that of uncharged polystyrene $b \approx 50$ Å ≥ 16 Å due to the contribution of intrachain electrostatic interactions.[53] Moreover, b decreases with concentration and approaches the bare value of a fully flexible chain.[32,54] As intended by our experimental design, we achieve comparable ξ values for solutions at different ionic strengths. Moreover, solutions with similar ξ have substantially different b values, indicating that the electrostatic interactions in these solutions are significantly different. From these structural measurements, we conclude that we have successfully produced a library of solutions in which geometric and electrostatic length scales are independently varied.

We now use these solutions to explicitly test how segmental relaxations depend on geometric and electrostatic length scales using NSE. Dynamic measurements are performed across a wide range of time scales 0.1 ns < t < 45 ns and wavevectors 0.051 Å^{-1} < Q < 0.26 Å^{-1}, equivalent to 0.45 < $Q\xi$ < 4.36. The normalized intermediate scattering functions are well-represented by a stretched exponential $I(Q, t)/I(Q, 0) = A\exp[(-\Gamma t)^{\beta}]$ (Figure 3a), where the prefactor $A = 1$ represents fully correlated dynamics at short t, β is the stretching exponent, and Γ is the relaxation rate characterizing segmental relaxations. The stretching exponent remains constant across the experimental wavevectors with an average value $\beta \approx 0.83 \pm 0.02$, indicating that chains follow Zimm-like relaxations. Although Zimm relaxations predict $\beta = 2/3$, over our range of interest, it has been found that $\beta \approx 0.85$.[55,56]

For neutral polymers that relax according to the Zimm model, the relaxation rate should scale with wavevector according to $\Gamma \sim Q^3$.[57] For these polyelectrolyte systems, however, there are two distinct scaling regions. At small length scales, the relaxation rates scale close to predictions (Figure 3b), but over longer length scales (small Q), the relaxation rates follow a weaker power law. The scaling behavior of the relaxation rate is qualitatively similar across all samples (SI). The transition between these two scaling regimes occurs at length scales comparable to Q^*, suggesting that the dynamic changes may arise from the structure of the solution. The different dynamic regimes are further emphasized when the relaxation rates are normalized according to their expected Q-dependence. Fundamentally, the correlation curves from NSE are related to the relative mean-squared displacement between polymer monomers according to a Gaussian approximation $I(Q, t)/I(Q, 0) = \exp[-\langle\Delta r^2(t)\rangle Q^2/6]$.[58] Following established methods,[59,60] we set this expression equal to the stretched exponential decays observed in our experiments, leading to $(\Gamma t)^{\beta} = -\langle\Delta r^2(t)\rangle Q^2/6$. Because polymer monomers move subdiffusively on these time scales ($\langle\Delta r^2(t)\rangle \sim t^{\beta}$), the relaxation rate must scale as $\Gamma \sim Q^{2/\beta}$.

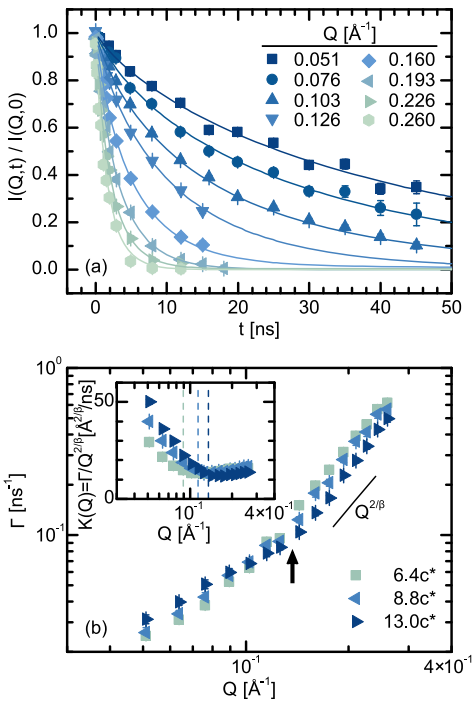

Figure 3. (a) Normalized intermediate scattering functions $I(Q, t)/I(Q, 0)$ as a function of Fourier time t at various values of the wavevectors Q for 6.4c^* NaPSS solution at 10^{-6} M ionic strength. (b) Relaxation rate Γ as a function of wavevector Q for NaPSS solutions at 10^{-6} M ionic strength. Inset: Relaxation rate normalized to length scales $\Gamma/Q^{2/\beta}$ for 10^{-6} M ionic strength solutions as a function of wavevector Q. Dashed lines represent the correlation peak length scale. Error bars are estimated according to a 95% confidence interval.

When normalized by $Q^{2/\beta}$, Γ decreases as a function of Q until it reaches a minimum at $Q \approx Q^*$, after which it increases to a constant value at large wavevector (inset of Figure 3b). This minimum shifts to higher Q with increasing polymer concentration, consistent with the shift in structure factor peak measured in SANS (Figure 2). These observations suggest that the structure of polyelectrolytes, mediated by the electrostatic repulsion between monomers, plays a significant role in dictating the chain dynamics.

Previous studies have reported suppressed dynamics across Q^* in multiarm polymers,[61,62] colloidal suspensions,[63−67] and particle−polymer composites.[60] In these systems, the dynamics can be interpreted through the phenomenon of de Gennes narrowing[35] in which a peak in the structure factor $S(Q)$ exists at Q^* due to the presence of a free energy minimum that slows relaxations. Under this framework, dynamics are inversely related to structure through $D(Q) \sim 1/S(Q)$, where $D(Q)$ is the wavevector-dependent diffusivity. An earlier study found that the diffusion coefficient of polyelectrolyte chains is inversely related to the structure.[68] In our solutions, however, we measure the segmental relaxations, which relax subdiffusively. Thus, we define an analogous subdiffusion coefficient that satisfies $\Gamma = KQ^{2/\beta}$, where K is a kinetic parameter that characterizes the subdiffusive Zimm relaxations in the system.

https://doi.org/10.1021/acsmacrolett.2c00213
ACS Macro Lett. 2022, 11, 854−860

To compare this kinetic parameter K to the structure of the solution, we must extract a structure factor $S(Q)$ from the measured scattering profiles. Typically, the scattering intensity can be decomposed according to $I(Q) = P(Q)S(Q)$, where $P(Q)$ is the form factor that captures the scattering from an individual component and $S(Q)$ is the structure factor that captures the scattering between components. Determining the unperturbed form factor $P(Q)$ for a polymer chain requires fitting the scattering intensity in the high-Q region where $S(Q) \rightarrow 1$. The complexity of the PRISM theory, however, prevents the fit from converging to physical values over this limited wavevector range. Therefore, we make a simplifying assumption that the polyelectrolyte chain structure can be represented as a perturbation from an ideal Gaussian chain.[44,69] To explore this picture, we fit the SANS scattering profile to a Lorentzian at high wavevectors ($Q \geq 0.3$ Å^{-1}), where $S(Q) \rightarrow 1$ for all real polymers, to represent $P(Q)$ of the Gaussian chains[70,71] according to

$$P(Q) = \frac{I_{poly}}{1 + (Q\xi_0)^2} \quad (2)$$

In this expression, I_{poly} is the scattering intensity of the polyelectrolyte chains and ξ_0 is the effective correlation length of the ideal, unperturbed chain. Because the monomer density is similar between solutions with the same correlation length ξ, we globally fit I_{poly} and ξ_0 across these samples. We then calculate $S(Q)$ of our NaPSS chains by dividing the total scattering $I(Q)$ from SANS by $P(Q)$ from eq 2. To evaluate the relationship between structure and dynamics in these semidilute polyelectrolyte solutions, we then compare these extracted $S(Q)$ to the normalized kinetic parameters $K_0/K(Q)$, where K_0 represents the dynamics in the absence of structural contributions. Following the procedure established in our earlier work,[60] K_0 is defined per sample at the wavevector at which $S(Q)$ is first equal to 1 after the peak. The $S(Q)$ curves capture the peak positions of $K_0/K(Q)$ at all NaPSS concentrations and ionic strengths (Figure 4a,b). Moreover, $S(Q)$ accurately predicts the trends of the dynamics before and after the structural peak. The weaker electrostatic repulsion at high ionic strength results in a shallower structural peak and less suppressed dynamics as the perturbation from a Gaussian chain becomes weaker (Figure 4b). Furthermore, $S(Q)$ still accurately captures the shape and decay of the dynamics as ionic strength changes. The excellent agreement between $S(Q)$ and K_0/K demonstrates that the segmental dynamics of polyelectrolytes are controlled in large part by their underlying structure. This observation demonstrates how electrostatics and concentration affect polyelectrolyte dynamics similarly to their effects on chain structure. Furthermore, the electrostatic repulsions that dictate the local structure in semidilute polyelectrolyte solutions also act to perturb the expected Zimm relaxations.

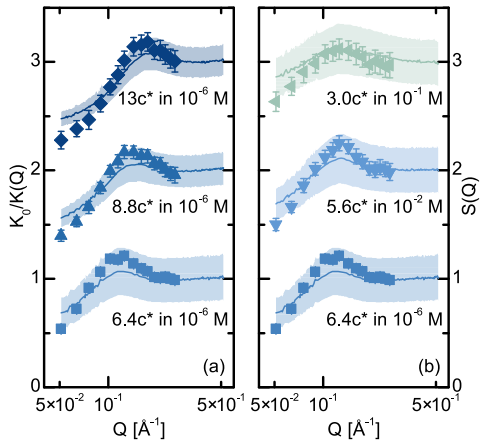

Figure 4. Normalized dynamic factor $K_0/K(Q)$ as a function of wavevector Q for NaPSS solutions (a) with different concentrations in 10^{-6} M solutions and (b) with a similar correlation length $\xi \sim 79$ Å at different ionic strengths. Solid lines represent the structure factor $S(Q)$ for the corresponding solution. Error bars are estimated according to a 95% confidence interval. The shaded region is a 95% confidence interval derived from a propagated error from the fitting of eq 2. Data and structure factors are shifted for clarity.

The success of our approach in relating the structure and dynamics of polyelectrolyte chains relies on the assumption that electrostatic interactions act as perturbations to a neutral chain. To implement this approach, we use the simplest model of an ideal chain. This implementation is necessary due to the extremely limited Q-range ($Q \geq 0.3$ Å^{-1}) over which we can fit $P(Q)$ in the absence of structural effects. As a result, the parameters from the fits to eq 2 do not fully describe the physics of our system. Whereas I_{poly} increases with polymer concentration as physically expected, the values of the effective correlation length ξ_0 converge to a constant (SI), irrespective of polymer concentration. We attribute this behavior to the inability of such a simple representation of the Laplacian form factor $P(Q)$ to capture subtle changes to polymer structure. An improved description of the relationship between structure and dynamics in these systems would require the development of a polyelectrolyte structure factor similar to those derived for colloidal suspensions.[72−74] Nevertheless, the excellent agreement between the observed dynamics and the calculated $S(Q)$ conclusively demonstrates that electrostatic repulsions suppress Zimm-like relaxations across the structural peak in semidilute polyelectrolyte solutions.

By independently varying the electrostatic and geometric length scales in semidilute solutions, we show that the dynamics of polyelectrolytes are strongly coupled to their structural properties in solutions. The polymer dynamics follow Zimm-like relaxations that are suppressed across the structure factor peak according to de Gennes narrowing. The extent to which dynamics are suppressed is directly correlated to the magnitude of structural changes due to electrostatics. Although our approach of determining the structure factor of polyelectrolytes uses the simplest model of Gaussian chains, we still observe remarkable agreement between structure and dynamics. We expect these findings to translate to other polyelectrolyte systems with different charge densities as counterion condensation changes structure by modifying the free energy landscape but should not affect the coupling between structure and dynamics. Additionally, NSE experiments have shown that bound counterions are dynamically correlated to polymer relaxation, suggesting that their dynamics might also be coupled to chain structure.[75] Our work illustrates the importance of incorporating the coupling between structure and dynamics to further understand polyelectrolyte chain properties. Developing structure−dynamics relationships is essential to accurately describe the properties of polyelectrolyte materials.

https://doi.org/10.1021/acsmacrolett.2c00213
ACS Macro Lett. 2022, 11, 854−860

■ ASSOCIATED CONTENT

Supporting Information

The Supporting Information is available free of charge at https://pubs.acs.org/doi/10.1021/acsmacrolett.2c00213.

Intrinsic viscosity and rheology measurements, estimates of chain length scales, Lorentzian fitting parameters, raw dynamics data, and detailed protocols of sample preparation, neutron scattering, and SANS fitting (PDF)

■ AUTHOR INFORMATION

Corresponding Authors

Amanda B. Marciel − *Department of Chemical and Biomolecular Engineering, Rice University, Houston, Texas 77005, United States*; Email: am152@rice.edu

Ryan Poling-Skutvik − *Department of Chemical Engineering, University of Rhode Island, Kingston, Rhode Island 02881, United States*; orcid.org/0000-0002-1614-1647; Email: ryanps@uri.edu

Jacinta C. Conrad − *Department of Chemical and Biomolecular Engineering, University of Houston, Houston, Texas 77204, United States*; orcid.org/0000-0001-6084-4772; Email: jcconrad@uh.edu

Authors

Ali H. Slim − *Department of Chemical and Biomolecular Engineering, University of Houston, Houston, Texas 77204, United States*

Winnie H. Shi − *Department of Chemical and Biomolecular Engineering, Rice University, Houston, Texas 77005, United States*; orcid.org/0000-0002-9310-8015

Farshad Safi Samghabadi − *Department of Chemical and Biomolecular Engineering, University of Houston, Houston, Texas 77204, United States*

Antonio Faraone − *National Institute of Standards and Technology Center for Neutron Research, Gaithersburg, Maryland 20899, United States*; orcid.org/0000-0002-3783-5816

Complete contact information is available at: https://pubs.acs.org/10.1021/acsmacrolett.2c00213

Notes

The authors declare no competing financial interest.

■ ACKNOWLEDGMENTS

We thank Megan Robertson for access to the rheometer. This research was partially supported by the National Science Foundation (CBET-2004652, CBET-2113767, and CBET-2113769), the Welch Foundation (E-1869 and C-2003-20190330), and the Rhode Island Foundation (Medical Research Award 3.2021). Access to NSE was provided by the Center for High Resolution Neutron Scattering, a partnership between the National Institute of Standards and Technology and the National Science Foundation under Agreement No. DMR-2010792. This work utilized SasView software, which was developed by the DANSE project from NSF Award DMR-0520547. Certain trade names and company products are identified in order to specify adequately the experimental procedure. In no case does such identification imply recommendation or endorsement by the National Institute of Standards and Technology, nor does it imply that the products are necessarily the best for the purpose.

■ REFERENCES

(1) Dobrynin, A. V. Theory and simulations of charged polymers: From solution properties to polymeric nanomaterials. *Curr. Opin. Colloid Interface Sci.* **2008**, *13*, 376−388.

(2) Horkay, F.; Basser, P. J.; Hecht, A.-M.; Geissler, E. Chondroitin Sulfate in Solution: Effects of Mono- and Divalent Salts. *Macromolecules* **2012**, *45*, 2882−2890.

(3) Geissler, E.; Hecht, A.-M.; Horkay, F. Scaling Behavior of Hyaluronic Acid in Solution with Mono- and Divalent Ions. *Macromol. Symp.* **2010**, *291*−*292*, 362−370.

(4) Janmey, P. A.; Slochower, D. R.; Wang, Y.-H.; Wen, Q.; Cēbers, A. Polyelectrolyte properties of filamentous biopolymers and their consequences in biological fluids. *Soft Matter* **2014**, *10*, 1439−1449.

(5) Yu, J.; Jackson, N. E.; Xu, X.; Morgenstern, Y.; Kaufman, Y.; Ruths, M.; De Pablo, J. J.; Tirrell, M. Multivalent counterions diminish the lubricity of polyelectrolyte brushes. *Science* **2018**, *360*, 1434−1438.

(6) Ammala, A. Biodegradable polymers as encapsulation materials for cosmetics and personal care markets. *Int. J. Cosmet. Sci.* **2013**, *35*, 113−124.

(7) Sakamoto, K.; Lochhead, R.; Maibach, H.; Yamashita, Y. *Cosmetic science and Technology: Theoretical Principles and Applications*; Elsevier, 2017.

(8) Meka, V. S.; Sing, M. K. G.; Pichika, M. R.; Nali, S. R.; Kolapalli, V. R. M.; Kesharwani, P. A comprehensive review on polyelectrolyte complexes. *Drug discovery today* **2017**, *22*, 1697−1706.

(9) Siyawamwaya, M.; Choonara, Y. E.; Bijukumar, D.; Kumar, P.; Du Toit, L. C.; Pillay, V. A Review: Overview of Novel Polyelectrolyte Complexes as Prospective Drug Bioavailability Enhancers. *Int. J. Polym. Mater. Polym. Biomater.* **2015**, *64*, 955−968.

(10) Thiele, M. J.; Davari, M. D.; Hofmann, I.; König, M.; Lopez, C. G.; Vojcic, L.; Richtering, W.; Schwaneberg, U.; Tsarkova, L. A. Enzyme-Compatible Dynamic Nanoreactors from Electrostatically Bridged Like-Charged Surfactants and Polyelectrolytes. *Angew. Chem., Int. Ed.* **2018**, *57*, 9402−9407.

(11) de Gennes, P.-G. *Scaling Concepts in Polymer Physics*; Cornell University Press: Ithaca, NY, 1979.

(12) de Gennes, P. G.; Pincus, P.; Velasco, R. M.; Brochard, F. Remarks on polyelectrolyte conformation. *J. Phys. (Paris)* **1976**, *37*, 1461−1473.

(13) Pfeuty, P. Conformation des polyélectrolytes ordre dans les solutions de polyélectrolytes. *J. Phys., Colloq.* **1978**, *39*, C2-149−C2-160.

(14) Dobrynin, A. V.; Colby, R. H.; Rubinstein, M. Scaling Theory of Polyelectrolyte Solutions. *Macromolecules* **1995**, *28*, 1859−1871.

(15) Carrillo, J.-M. Y.; Dobrynin, A. V. Polyelectrolytes in Salt Solutions: Molecular Dynamics Simulations. *Macromolecules* **2011**, *44*, 5798−5816.

(16) Muthukumar, M. 50th Anniversary Perspective: A Perspective on Polyelectrolyte Solutions. *Macromolecules* **2017**, *50*, 9528−9560.

(17) Colby, R. H. Structure and linear viscoelasticity of flexible polymer solutions: Comparison of polyelectrolyte and neutral polymer solutions. *Rheol. Acta* **2010**, *49*, 425−442.

(18) Rubinstein, M.; Colby, R. H.; Dobrynin, A. V. Dynamics of Semidilute Polyelectrolyte Solutions. *Phys. Rev. Lett.* **1994**, *73*, 2776.

(19) Krause, W. E.; Tan, J. S.; Colby, R. H. Semidilute solution rheology of polyelectrolytes with no added salt. *J. Polym. Sci. B Polym. Phys.* **1999**, *37*, 3429−3437.

(20) Jacobs, M.; Lopez, C. G.; Dobrynin, A. V. Quantifying the Effect of Multivalent Ions in Polyelectrolyte Solutions. *Macromolecules* **2021**, *54*, 9577−9586.

(21) Lopez, C. G.; Horkay, F.; Mussel, M.; Jones, R. L.; Richtering, W. Screening lengths and osmotic compressibility of flexible polyelectrolytes in excess salt solutions. *Soft Matter* **2020**, *16*, 7289−7298.

(22) Lopez, C. G. Entanglement Properties of Polyelectrolytes in Salt-Free and Excess-Salt Solutions. *ACS Macro Lett.* **2019**, *8*, 979−983.

(23) Zimm, B. H. Dynamics of Polymer Molecules in Dilute Solution: Viscoelasticity, Flow Birefringence and Dielectric Loss. *J. Chem. Phys.* **1956**, *24*, 269.
(24) Rouse, P. E. A. Theory of the Linear Viscoelastic Properties of Dilute Solutions of Coiling Polymers. *J. Chem. Phys.* **1953**, *21*, 1272.
(25) de Gennes, P. G. Reptation of a Polymer Chain in the Presence of Fixed Obstacles. *J. Chem. Phys.* **1971**, *55*, 572.
(26) Noda, I.; Takahashi, Y. Viscoelastic properties of polyelectrolyte solutions. *Berichte der Bunsengesellschaft für physikalische Chemie* **1996**, *100*, 696−702.
(27) Boris, D. C.; Colby, R. H. Rheology of sulfonated polystyrene solutions. *Macromolecules* **1998**, *31*, 5746−5755.
(28) Di Cola, E.; Plucktaveesak, N.; Waigh, T. A.; Colby, R. H.; Tan, J. S.; Pyckhout-Hintzen, W.; Heenan, R. K. Structure and Dynamics in Aqueous Solutions of Amphiphilic Sodium Maleate-Containing Alternating Copolymers. *Macromolecules* **2004**, *37*, 8457−8465.
(29) Dou, S.; Colby, R. H. Charge density effects in salt-free polyelectrolyte solution rheology. *J. Polym. Sci., Part B: Polym. Phys.* **2006**, *44*, 2001−2013.
(30) Liao, Q.; Carrillo, J.-M. Y.; Dobrynin, A. V.; Rubinstein, M. Rouse Dynamics of Polyelectrolyte Solutions: Molecular Dynamics Study. *Macromolecules* **2007**, *40*, 7671−7679.
(31) Dou, S.; Colby, R. H. Solution Rheology of a Strongly Charged Polyelectrolyte in Good Solvent. *Macromolecules* **2008**, *41*, 6505−6510.
(32) Lopez, C. G.; Richtering, W. Conformation and dynamics of flexible polyelectrolytes in semidilute salt-free solutions. *J. Chem. Phys.* **2018**, *148*, 244902.
(33) Lopez, C. G.; Richtering, W. Viscosity of Semidilute and Concentrated Nonentangled Flexible Polyelectrolytes in Salt-Free Solution. *J. Phys. Chem. B* **2019**, *123*, 5626−5634.
(34) Muthukumar, M. Collective dynamics of semidilute polyelectrolyte solutions with salt. *J. Polym. Sci., Part B: Polym. Phys.* **2019**, *57*, 1263−1269.
(35) de Gennes, P. G. Liquid dynamics and inelastic scattering of neutrons. *Physica* **1959**, *25*, 825−839.
(36) Hong, L.; Smolin, N.; Smith, J. C. de Gennes Narrowing Describes the Relative Motion of Protein Domains. *Phys. Rev. Lett.* **2014**, *112*, 158102.
(37) Slim, A. H.; Poling-Skutvik, R.; Conrad, J. C. Local Confinement Controls Diffusive Nanoparticle Dynamics in Semidilute Polyelectrolyte Solutions. *Langmuir* **2020**, *36*, 9153−9159.
(38) Glinka, C. J.; Barker, J. G.; Hammouda, B.; Krueger, S.; Moyer, J. J.; Orts, W. J. The 30 m Small-Angle Neutron Scattering Instruments at the National Institute of Standards and Technology. *J. Appl. Crystallogr.* **1998**, *31*, 430−445.
(39) Barker, J. G.; Glinka, C. J.; Moyer, J. J.; Kim, M. H.; Drews, A. R.; Agamalian, M. Design and performance of a thermal-neutron double-crystal diffractometer for USANS at NIST. *J. Appl. Crystallogr.* **2005**, *38*, 1004−1011.
(40) Kline, S. R. Reduction and analysis of SANS and USANS data using IGOR Pro. *J. Appl. Crystallogr.* **2006**, *39*, 895−900.
(41) Azuah, R. T.; Kneller, L. R.; Qiu, Y.; Tregenna-Piggott, P. L. W.; Brown, C. M.; Copley, J. R. D.; Dimeo, R. M. DAVE: A Comprehensive Software Suite for the Reduction, Visualization, and Analysis of Low Energy Neutron Spectroscopic Data. *J. Res. Natl. Inst. Stand. Technol.* **2009**, *114*, 341−358.
(42) Richter, D.; Binder, K.; Ewen, B.; St uhn, B. Screening of Hydrodynamic Interactions in Dense Polymer Solutions: A Phenomenological Theory and Neutron-Scattering Investigations. *J. Phys. Chem.* **1984**, *88*, 6618−6633.
(43) Rubinstein, M.; Colby, R. H. *Polymer Physics*; Oxford University Press: New York, 2003.
(44) Josef, E.; Bianco-Peled, H. Conformation of a natural polyelectrolyte in semidilute solutions with no added salt. *Soft Matter* **2012**, *8*, 9156−9165.
(45) Pedersen, J. S.; Schurtenberger, P. Scattering Functions of Semiflexible Polymers with and without Excluded Volume Effects. *Macromolecules* **1996**, *29*, 7602−7612.
(46) Chen, W.-R.; Butler, P. D.; Magid, L. J. Incorporating Intermicellar Interactions in the Fitting of SANS Data from Cationic Wormlike Micelles. *Langmuir* **2006**, *22*, 6539−6548.
(47) Schweizer, K. S.; David, E. F.; Singh, C.; Curro, J. G.; Rajasekaran, J. J. Structure-Property Correlations of Atomistic and Coarse-Grained Models of Polymer Melts. *Macromolecules* **1995**, *28*, 1528−1540.
(48) Pedersen, J. S.; Schurtenberger, P. Scattering Functions of Semidilute Solutions of Polymers ina Good Solvent. *J. Polym. Sci. B Polym. Phys.* **2004**, *42*, 3081−3094.
(49) Pedersen, J. S.; Schurtenberger, P. Static properties of polystyrene in semidilute solutions: A comparison of Monte Carlo simulation and small-angle neutron scattering results. *Europhys. Lett.* **1999**, *45*, 666−672.
(50) Arleth, L.; Bergström, M.; Pedersen, J. S. Small-Angle Neutron Scattering Study of the Growth Behavior, Flexibility, and Intermicellar Interactions of Wormlike SDS Micelles in NaBr Aqueous Solutions. *Langmuir* **2002**, *18*, 5343−5353.
(51) Marciel, A. B.; Srivastava, S.; Tirrell, M. V. Structure and rheology of polyelectrolyte complex coacervates. *Soft Matter* **2018**, *14*, 2454−2464.
(52) Dobrynin, A. V.; Rubinstein, M. Theory of polyelectrolytes in solution and at surfaces. *Prog. Polym. Sci.* **2005**, *30*, 1049−1118.
(53) Bershtein, V. A.; Egorov, V. M. *Differential Scanning Calorimetry of Polymers: Physics, Chem-istry, Analysis, Technology*; Ellis Horwood: New York, 1994.
(54) Lopez, C. G.; Colby, R. H.; Graham, P.; Cabral, J. T. Viscosity and Scaling of Semiflexible Polyelectrolyte NaCMC in Aqueous Salt Solutions. *Macromolecules* **2017**, *50*, 332−338.
(55) Richter, D.; Monkenbusch, M.; Arbe, A.; Colmenero, J. Neutron Spin Echo in Polymer Systems. *Advances in Polymer Science*; Springer: Berlin, Heidelberg, 2005; Vol. *174*.
(56) Ewen, B.; Richter, D. Neutron Spin Echo Investigations on the Segmental Dynamics of Polymers in Melts, Networks and Solutions. Neutron Spin Echo Spectroscopy Viscoelasticity Rheology. *Advances in Polymer Science*; Springer: Berlin, Heidelberg, 1997; Vol. *134*.
(57) Monkenbusch, M. In *Neutron Spin Echo Spectroscopy - Basics, Trends and Applications*; Mezei, F., Pappas, C., Gutberlet, T., Eds.; Springer: Berlin, 2003; pp 246−265.
(58) Smith, G. D.; Paul, W.; Monkenbusch, M.; Richter, D. On the non-Gaussianity of chain motion in unentangled polymer melts. *J. Chem. Phys.* **2001**, *114*, 4285−4288.
(59) Guo, H.; Bourret, G.; Lennox, R. B.; Sutton, M.; Harden, J. L.; Leheny, R. L. Entanglement-Controlled Subdiffusion of Nanoparticles within Concentrated Polymer Solutions. *Phys. Rev. Lett.* **2012**, *109*, 055901.
(60) Poling-Skutvik, R.; Mongcopa, K. I. S.; Faraone, A.; Narayanan, S.; Conrad, J. C.; Krishnamoorti, R. Structure and Dynamics of Interacting Nanoparticles in Semidilute Polymer Solutions. *Macromolecules* **2016**, *49*, 6568−6577.
(61) Richter, D.; Farago, B.; Fetters, L. J.; Huang, J. S.; Ewen, B. On the Relation between Structure and Dynamics of Star Polymers in Dilute Solution. *Macromolecules* **1990**, *23*, 1845−1856.
(62) Vlassopoulos, D.; Pakula, T.; Fytas, G.; Roovers, J.; Karatasos, K.; Hadjichristidis, N. Ordering and viscoelastic relaxation in multiarm star polymer melts. *Europhys. Lett.* **1997**, *39*, 617−622.
(63) Segrè, P. N.; Behrend, O. P.; Pusey, P. N. Short-time Brownian motion in colloidal suspensions: Experiment and simulation. *Phys. Rev. E* **1995**, *52*, 5070−5083.
(64) Segrè, P. N.; Pusey, P. N. Scaling of the Dynamic Scattering Function of Concentrated Colloidal Suspensions. *Phys. Rev. Lett.* **1996**, *77*, 771−774.
(65) Holmqvist, P.; Nägele, G. Long-Time Dynamics of Concentrated Charge-Stabilized Colloids. *Phys. Rev. Lett.* **2010**, *104*, 058301.
(66) Sikorski, M.; Sandy, A. R.; Narayanan, S. Depletion-Induced Structure and Dynamics in Bimodal Colloidal Suspensions. *Phys. Rev. Lett.* **2011**, *106*, 188301.

https://doi.org/10.1021/acsmacrolett.2c00213
ACS Macro Lett. 2022, 11, 854−860

(67) Hoshino, T.; Kikuchi, M.; Murakami, D.; Harada, Y.; Mitamura, K.; Ito, K.; Tanaka, Y.; Sasaki, S.; Takata, M.; Jinnai, H.; Takahara, A. X-ray photon correlation spectroscopy using a fast pixel array detector with a grid mask resolution enhancer. *J. Synchrotron Rad.* **2012**, *19*, 988−993.
(68) Hayter, J.; Janninck, G.; Brochard-Wyart, F.; de Gennes, P. G. Correlations and dynamics of polyelectrolyte solutions. *J. Phys. Lett. (Paris)* **1980**, *41*, 451−454.
(69) Sayko, R.; Tian, Y.; Liang, H.; Dobrynin, A. V. Charged Polymers: From Polyelectrolyte Solutions to Polyelectrolyte Complexes. *Macromolecules* **2021**, *54*, 7183−7192.
(70) Cotton, J. P.; Nierlich, M.; Boué, F.; Daoud, M.; Farnoux, B.; Jannink, G.; Duplessix, R.; Picot, C. Experimental determination of the temperature−concentration diagram of flexible polymer solutions by neutron scattering. *J. Chem. Phys.* **1976**, *65*, 1101.
(71) Pezron, I.; Djabourov, M.; Leblond, J. Conformation of gelatin chains in aqueous solutions: 1. A light and small-angle neutron scattering study. *Polymer* **1991**, *32*, 3201−3210.
(72) Hayter, J. B.; Penfold, J. An analytic structure factor for macroion solutions. *Mol. Phys.* **1981**, *42*, 109−118.
(73) Hansen, J.-P.; Hayter, J. B. A rescaled MSA structure factor for dilute charged colloidal dispersions. *Mol. Phys.* **1982**, *46*, 651−656.
(74) Mildner, D. F. R.; Hall, P. L. Small-angle scattering from porous solids with fractal geometry. *J. Phys. D: Appl. Phys.* **1986**, *19*, 1535−1545.
(75) Prabhu, V. M.; Amis, E. J.; Bossev, D. P.; Rosov, N. Counterion associative behavior with flexible polyelectrolytes. *J. Chem. Phys.* **2004**, *121*, 4424−4429.

https://doi.org/10.1021/acsmacrolett.2c00213
ACS Macro Lett. 2022, 11, 854−860